

Comparison of radiocarbon and OSL dating methods for a Late Quaternary sediment core from Lake Ulaan, Mongolia

Min Kyung Lee · Yong Il Lee · Hyoun Soo Lim ·
Jae Il Lee · Jeong Heon Choi · Ho Il Yoon

Received: 9 August 2010/Accepted: 30 November 2010/Published online: 14 December 2010
© Springer Science+Business Media B.V. 2010

Abstract Both radiocarbon and optically stimulated luminescence (OSL) dating methods were applied to test their suitability for establishing a chronology of arid-zone lacustrine sediments using a 5.88-m-long core drilled from Lake Ulaan, southern Mongolia. Although the radiocarbon and OSL ages agree in some samples, the radiocarbon ages are older than the corresponding OSL ages at the 550-cm depth horizon (late Pleistocene) and in the 100–300-cm interval (early to late Holocene). In the early to late Holocene, radiocarbon ages are consistently older than OSL ages by 4,100–5,800 years, and in the late Pleistocene by 2,700–3,000 years. Grain-size analysis of early to late Holocene sediments and one late Pleistocene sediment sample (550-cm depth) indicates that eolian processes were the dominant sediment-transport mechanism. Also, two late Pleistocene sediments samples (from 400- to 500-cm depths) are

interpreted to have been deposited by both eolian and glaciofluvial processes. Accordingly, the radiocarbon ages that were older than the corresponding OSL ages during the Holocene seem to have been a consequence of the influx of ^{14}C -deficient carbon delivered from adjacent soils and Paleozoic carbonate rocks by the westerly winds, a process that is also active today. In addition to the input of old reworked carbon by eolian processes, the late Pleistocene sediments were also influenced by old carbon delivered by deglacial meltwater. The results of this study suggest that when eolian sediment transport is suspected, especially in lakes of arid environments, the OSL dating method is superior to the radiocarbon dating method, as it eliminates a common ‘old-carbon’ error problem.

Keywords Radiocarbon · OSL · Lacustrine sediment · Arid condition · Mongolia

M. K. Lee · Y. I. Lee (✉)
School of Earth and Environmental Sciences,
Seoul National University, Seoul 151-747, Korea
e-mail: lee2602@plaza.snu.ac.kr

M. K. Lee · H. S. Lim · J. I. Lee · H. I. Yoon
Korea Polar Research Institute, KORDI,
Incheon 406-840, Korea

J. H. Choi
Division of Earth and Environmental Sciences,
Korea Basic Science Institute, Daejeon 305-333, Korea

Introduction

Accurate chronologies are of crucial importance in paleoclimatic and paleoenvironmental studies of lake sediments. Lake sediments usually contain a certain amount of organic carbon and are therefore suitable for radiocarbon dating. Since its discovery, radiocarbon dating has become the most widely applied chronological tool in the study of late Quaternary

lake sediment sequences. However, the applicability of radiocarbon dating methods in lake sediments with low organic carbon content and a lack of macrofossils is limited. Also, a common problem encountered in radiocarbon dating of limnic sediments is an ‘old-carbon’ error, caused by contamination from old reworked carbon, in which the samples are deficient in ^{14}C relative to the isotopic composition in the atmosphere at the time of deposition. The uncertainties of old-carbon contamination have raised serious concerns about radiocarbon dating of lake sediments, particularly in regions where calcareous bedrock is present (Karrow and Anderson 1975; Clayton and Moran 1982; Fowler et al. 1986; MacDonald et al. 1987; Aravena et al. 1992).

Recently, the optically stimulated luminescence (OSL) dating technique has also been applied to lake sediments (Shen et al. 2007; Liu et al. 2010; Zhao et al. 2010; Long et al. 2011 and references therein). The OSL method is exempt from ‘old-carbon’ problems commonly encountered in radiocarbon dating and can be a reliable tool for dating sediments if samples are well exposed to sunlight. This study compares the results of the above two dating methods, radiocarbon and OSL dating, applied to the lake sediment deposited in an arid environment. The results of this study should inform the selection of a better dating method when dealing with lacustrine sediments affected by eolian processes.

Study site

The studied lake, Lake Ulaan, is located in southern Mongolia, near the Gobi-Altai Mountains, about 120 km northwest of Dalanzadgad, Omnogovi Province (Fig. 1). Lake Ulaan occupied about 65 km² in the 1960s, but at present, the lake bottom is exposed. It is the easternmost lake of the lakes of the Gobi Valley and is known to have been fed by the Ongin Gol (Ongin River), which originates from the Khangai Mountains. The Ongin River has shrunk and has not supplied water to the lake since the mid-1990s. The present climate of the Lake Ulaan region is arid and continental. The average annual rainfall in the lake basin area is about 100–150 mm. Due to the presence of the Siberian High which guards the westerly approaches to Mongolia, a high pressure system is frequent over the country all year round, and westerly and southwesterly winds are dominant in the study region. The orientation and shape of partially vegetated sand dunes near the northern margin of the lake confirm the prevalence of westerly winds during the recent past. Our field study reveals that hills to the west and south of the lake are composed mainly of Silurian limestone/dolomite and Cretaceous basalt and clastic sedimentary rocks. To the east and north, the bedrock is dominated by Archaean and Paleoproterozoic metamorphic complex and Paleozoic–Mesozoic sedimentary rocks.

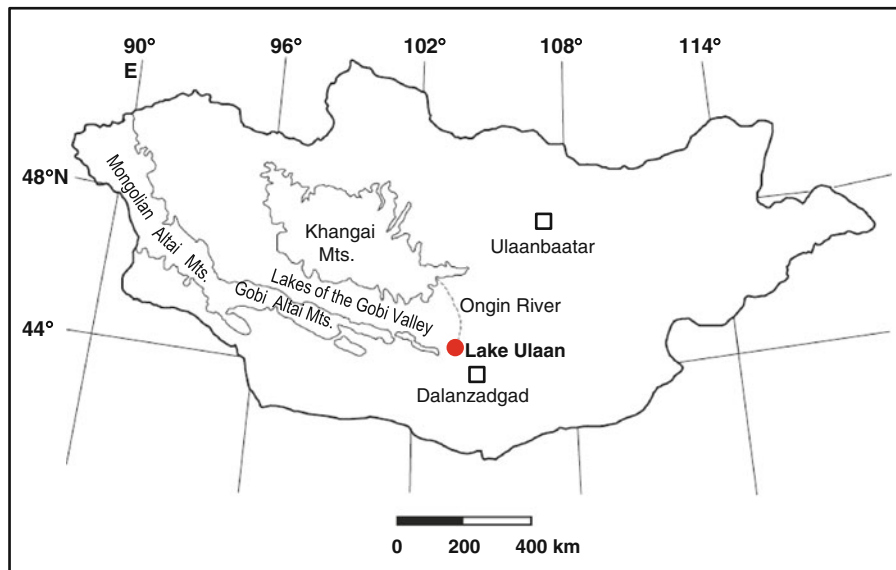


Fig. 1 Map of Mongolia showing the location of *Lake Ulaan*

Methods

Field methods

A 5.88-m-long core (ULB) was collected from the southern part of Lake Ulaan ($44^{\circ}30'50.1''N$, $103^{\circ}39'16.0''E$) in July 2007. We used a piston corer with several brass tubes of 76 mm in outer diameter and 74 mm in inner diameter. No detectable disconformities were identified in this core, suggesting a continuous sedimentation from the bottom to the core top.

Grain-size analysis

One hundred and forty-seven samples taken at 4-cm intervals from the ULB core were dried in an oven at $105^{\circ}C$ for 2 days. About 5 g of subsamples were reacted with H_2O_2 solution for 1 day to remove organic matter. After H_2O_2 was added, the H_2O_2 solution with sample was boiled for 1 h to further remove any remaining organic matter. Grain-size distribution of the fraction larger than 63 μm (sand and gravel) was determined by wet sieving. For the fine fraction smaller than 63 μm (clay and silt), samples were settled in an 1,000-ml graduated cylinder for 3 days, and the grain size was determined using Micrometrics Sedigraph 5100. Raw data were processed after Jones et al. (1988).

Radiocarbon dating

Seventeen bulk samples were collected from the longitudinal half of the ULB core for radiocarbon dating, with a sample interval of 12–50 cm. After examining subsamples under a microscope and picking out plant fragments with tweezers, bulk samples were pulverized using a mortar and pestle and sieved through 150- μm sieve. Sieved samples were treated by acid–alkali–acid processes (0.5 M HCl—0.1 M NaOH/0.1 M $Na_4P_2O_7$ —0.5 M HCl), and dried in a vacuum oven. Accelerated mass spectrometry (AMS) ^{14}C dating of these bulk samples was performed at the Rafter Radiocarbon Laboratory of the Institute of Geological and Nuclear Sciences, New Zealand, and the results are given as percent modern carbon (pmc) based on the National Institute of Standards and Technology (NIST) oxalic acid ($HOxI$) standard corrected for decay since 1950. All radiocarbon dates were calibrated to calendar years

using the IntCal09 dataset from Reimer et al. (2009) by means of the OxCal 4.1 (Bronk Ramsey 2009; Table 1) after $^{13}C/^{12}C$ adjustment.

Optically stimulated luminescence dating

Twelve samples were taken from the other longitudinal half of the core under subdued red-light conditions with a 50-cm depth interval. Analysis was carried out at the Korea Basic Science Institute. The outer part of each sample near the surface of the split core and the contact with the core liner was carved out to avoid possible incorporation of mineral grains that might have been exposed to sunlight during sampling and core cutting. The 4–11- μm fractions were separated by Stoke's Law of settling, and pure quartz grains were then recovered from this size fraction through a sequential use of HCl (10%, for 6 h) to dissolve carbonates, H_2O_2 (10%, for 24 h) to remove organic materials, and H_2SiF_6 (40%, for 14 days) to remove feldspar grains. Quartz OSL signals were measured using a Risø TL/OSL automated system (Bøtter-Jensen et al. 2000), and the SAR (single-aliquot regenerative-dose) protocol (Murray and Wintle 2000; 2003) was used to estimate equivalent dose (D_e) values. A blue LED array delivering 40 mW cm^{-2} was used as a stimulation light source, and signal detection was made through a 7-mm Hoya U-340 filter. A $^{90}Sr/^{90}Y$ beta source (80 mCi, dose rate to sample position: $\sim 0.216 \pm 0.008 \text{ Gy s}^{-1}$) was used for laboratory irradiation. A high-resolution gamma spectrometer was used to measure the radioactive element concentrations of the samples (Murray et al. 1987), which were then converted to dose rates using the data presented by Olley et al. (1996). α value was assumed to be 0.04 (Rees-Jones 1995), and a beta attenuation factor of 0.93 ± 0.03 was used for dose-rate calculation. All dose rates were modified using present water contents and the attenuation factors given by Zimmerman (1971). Cosmic ray contributions were calculated using the equations given in Prescott and Hutton (1988, 1994).

Results

Grain-size distribution

The ULB core sediments can be divided into three units based on grain-size distribution (Fig. 2a): unit 1

Table 1 Radiocarbon dating results of sediment samples collected from Lake Ulaan, Mongolia

Sample code	Lab. code	Depth (cm)	Material	$\delta^{13}\text{C}$	^{14}C age (year BP)	Calibrated age ranges 2σ (year BP)	Point estimate (year BP)
ULB1-50S	NZA30880	50	Bulk sediment	−32.4	5,982 ± 45	6,944–6,697	6,820
ULB2-100S	NZA30881	100	Bulk sediment	−29.1	6,035 ± 35	6,981–6,788	6,879
ULB3-150S	NZA30876	150	Bulk sediment	−24.8	8,390 ± 50	9,521–9,293	9,406
ULB3-200S	NZA30879	200	Bulk sediment	−25.5	9,894 ± 50	11,601–11,207	11,316
ULB4-250S	NZA30877	250	Bulk sediment	−30.0	10,541 ± 60	12,637–12,222	12,478
ULB4-300S	NZA30882	300	Bulk sediment	−28.1	12,295 ± 60	14,880–13,954	14,297
ULB5-350S	NZA30883	350	Bulk sediment	−25.9	10,331 ± 45	12,389–12,002	12,186
ULB5-356S	NZA30778	356	Bulk sediment	−28.6	9,471 ± 35	11,065–10,588	10,733
ULB6-368S	NZA30777	368	Bulk sediment	−27.0	8,468 ± 30	9,533–9,453	9,493
ULB6-400S	NZA30907	400	Bulk sediment	−26.0	12,363 ± 60	14,915–14,051	14,432
ULB6-414S	NZA30878	414	Bulk sediment	−31.3	10,270 ± 190	12,569–11,353	11,988
ULB7-450S	NZA30885	450	Bulk sediment	−37.0	15,300 ± 210	18,891–18,002	18,472
ULB7-455S	NZA30886	455	Bulk sediment	−38.4	19,780 ± 220	24,316–22,972	23,638
ULB7-500S	NZA30887	500	Bulk sediment	−31.9	13,830 ± 200	17,522–16,525	16,965
ULB8-528S	NZA30888	528	Bulk sediment	−30.8	12,960 ± 210	16,673–14,860	15,683
ULB8-550S	NZA30889	550	Bulk sediment	−28.5	15,280 ± 210	18,877–17,996	18,449
ULB8-559S	NZA30779	559	Bulk sediment	−36.4	20,840 ± 110	25,157–24,462	24,816
ULB8-571S	NZA30903	571	Bulk sediment	−39.1	22,800 ± 130	28,014–26,920	27,501

(0–392 cm), unit 2 (392–530 cm), and unit 3 (530–588 cm). Unit 1 sediments are mainly composed of silt and clay, and they are moderately to poorly sorted (Fig. 2b). Their grain-size distribution is almost unimodal between 8 and 12 φ (about 0.25–4 μm) (Fig. 2c) except sediments of the interval from the core top down to 64 cm. This top core interval contains weakly consolidated pedogenic calcite concretions, and the mean grain size fluctuates between 6 and 9 φ with very poor sorting (2 to 2.6 φ). In contrast, unit 2 sediments consist of sand and clay and are very poorly sorted ($\sim 3 \varphi$). They show a distinctive bimodal grain-size distribution, with modes between 2 and 4 φ (63–250 μm) and between 8 and 12 φ (0.25–4 μm), with the coarser fraction being more abundant than the finer (Fig. 2c). As the relative amount of coarser fraction changes with time, the mean grain size fluctuates between about 6 and 8 φ within unit 2. Unit 3 sediments are dominated by clays with some sands, and they show a weak bimodal size distribution. Sediments are poorly to very poorly sorted.

AMS ^{14}C ages

The radiocarbon age data from the ULB core sediments are summarized in Table 1 and shown in Fig. 3. The calibrated ages lie in the range of 6,800–27,500 cal years BP. The weighted average of the probability distribution function is used as a point estimate of each calibrated date range (Telford et al. 2004). Radiocarbon ages show a linearly increasing trend in the upper part (from top to 300-cm depth) with a relatively narrow range of $\delta^{13}\text{C}$ values, whereas in the lower part (350-cm depth to the core bottom), they are somewhat scattered with fluctuating $\delta^{13}\text{C}$ values. Also, ages are stratigraphically reversed between 300 and 350-cm depth horizons. Considering that the $\delta^{13}\text{C}$ values of C_3 plants are generally between about −22 and −34‰ (Schidlowski et al. 1983), four samples at 450-, 455-, 559-, and 571-cm depths with largely negative $\delta^{13}\text{C}$ values (−36.4 to −39.1‰) may indicate the influence of old carbon. Thus, in this paper, only data whose $\delta^{13}\text{C}$ values are larger than −34‰ (marked with

Fig. 2 The results of grain-size analysis of the ULB core. **a** Mean grain size versus depth. Grain-size distribution of units 1 and 3 is shown in **(b)** and that of unit 2 in **(c)**

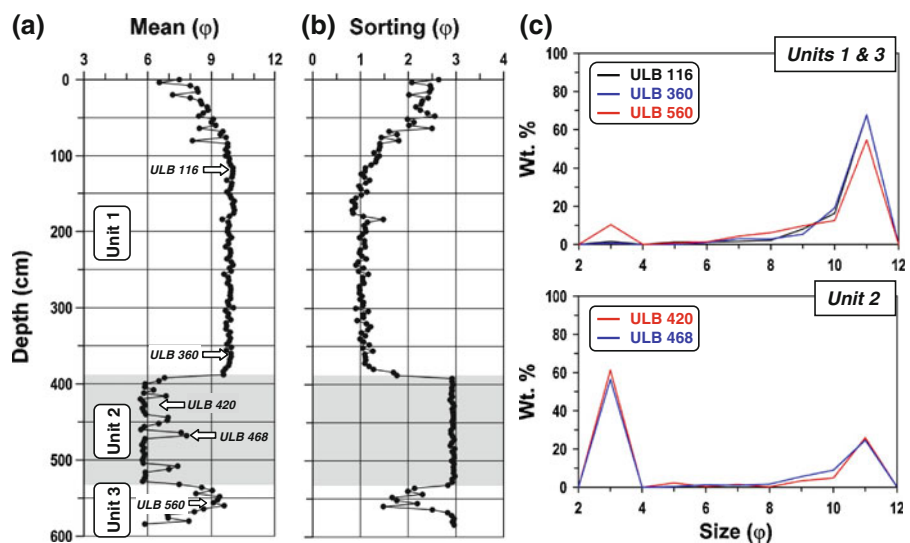
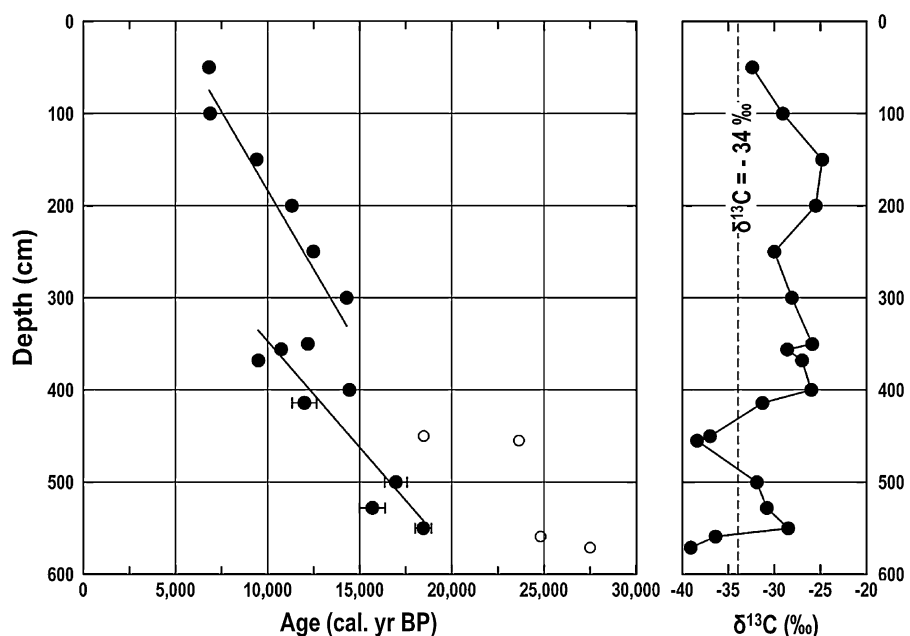


Fig. 3 Radiocarbon age and $\delta^{13}\text{C}$ values versus depth. Depth is given in cm below the core top. Only radiocarbon ages with $\delta^{13}\text{C}$ values greater than $-34\text{\textperthousand}$ are considered to be meaningful, and the rest are expressed as open circles



filled circles in Fig. 3) were used to establish a chronology. Except for these four samples, the radiocarbon age results were defined by two regression lines with different gradients (upper part: $Y = 0.034X - 158.735$, $r^2 = 0.83$; lower part: $Y = 0.023X + 116.689$, $r^2 = 0.81$).

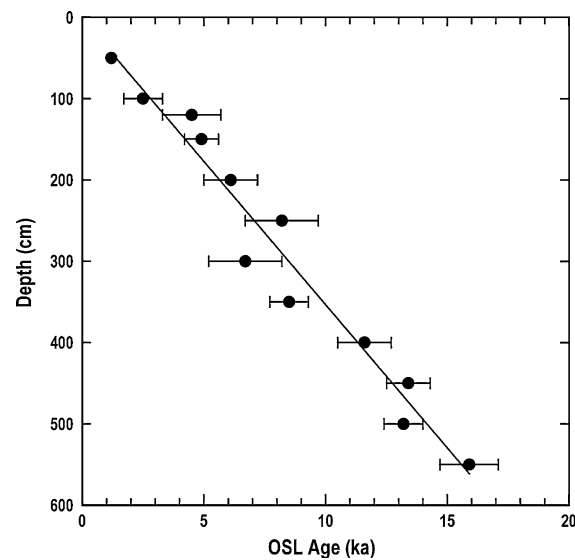
OSL ages

Table 2 shows the D_e , age, radionuclide concentrations, dose rate, and present water content of the

studied samples. The natural OSL signals in quartz grains from all the samples were observed to be far under the dose saturation level; all the quartz D_e values were far lower than $2D_0$ values (characteristic dose: Wintle and Murray 2006) of the dose-response growth curves. The observed water-content variations are partially related to grain size and sediment type. The quartz OSL ages of samples all fall in the range between 1.2 and 15.9 ka and are plotted against depth in Fig. 4. OSL age results are stratigraphically consistent in spite of larger error

Table 2 OSL dating results and summary of dosimetry

Sample code	Depth (cm)	Dose rate (Gy/ka)	Water content (%) ^a	Equivalent dose (Gy)	Aliquots used (<i>n</i>)	OSL age (ka, SD) ^b
ULO-50	50	3.62 ± 0.05	13.1 ± 1.1	4.5 ± 0.5	46	1.2 ± 0.1
ULO-100	100	3.87 ± 0.04	19.0 ± 0.0	9.6 ± 3.2	34	2.5 ± 0.8
ULO-120	120	3.79 ± 0.07	19.6 ± 0.0	16.9 ± 4.6	30	4.5 ± 1.2
ULO-150	150	3.93 ± 0.11	20.2 ± 0.0	19.4 ± 2.8	47	4.9 ± 0.7
ULO-200	200	3.03 ± 0.06	26.0 ± 0.5	18.5 ± 3.3	47	6.1 ± 1.1
ULO-250	250	3.09 ± 0.06	25.9 ± 0.2	25.2 ± 4.7	48	8.2 ± 1.5
ULO-300	300	3.60 ± 0.15	27.9 ± 4.8	24.0 ± 5.3	48	6.7 ± 1.5
ULO-350	350	2.97 ± 0.09	26.8 ± 0.9	25.2 ± 2.2	48	8.5 ± 0.8
ULO-400	400	2.99 ± 0.08	16.2 ± 0.7	34.8 ± 3.1	48	11.6 ± 1.1
ULO-450	450	2.99 ± 0.09	18.0 ± 1.2	40.1 ± 2.4	48	13.4 ± 0.9
ULO-500	500	3.10 ± 0.09	14.0 ± 0.5	41.0 ± 2.0	48	13.2 ± 0.8
ULO-550	550	2.75 ± 0.09	25.3 ± 1.9	43.7 ± 3.0	48	15.9 ± 1.2

^a The present water content^b Standard deviation**Fig. 4** OSL age versus depth. Depth is given in cm below the core top

ranges compared with radiocarbon ages. Most OSL ages are shown to define a good regression line, $Y = 0.035X + 1.108$ ($r^2 = 0.96$).

Discussion

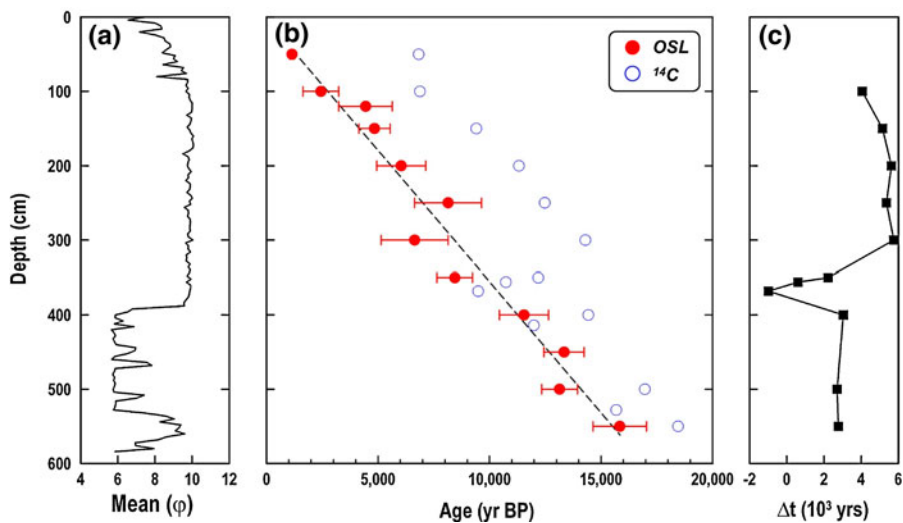
Unit 1 (0–392 cm) and unit 3 (530–588 cm) sediments are characterized by unimodal grain-size distribution and very fine grain size (0.25–4 μm).

Considering the small lake size and lake-level fluctuations in a closed lake, it is difficult to interpret that the thick, homogeneous, very fine sediments in units 1 and 3 were deposited in the lake under the influence of fluvial processes. Accordingly, units 1 and 3 sediments are interpreted to have been primarily transported to the lake by eolian processes.

On the other hand, in the case of unit 2 (latest Pleistocene), which is characterized by bimodal size distribution and very poor sorting, sediments were transported by a transport mechanism other than wind. In the late Pleistocene, a huge paleolake, which included Lake Ulaan, Lake Bon Cagaan, Lake Adagin Cagaan, and Lake Orog, was fed by thawed snow derived from mountain glaciers in the Gobi Altai and/or Khangai Mountains (Sevastyanov and Dorofeyk 2005). Accordingly, unit 2 sediments are interpreted to have been deposited by a combination of eolian and glaciofluvial processes. The fluctuation of mean grain size indicates that the meltwater inflow was intermittent.

The radiocarbon and OSL ages are plotted against depth in Fig. 5. Bulk ^{14}C ages and OSL ages appear to be almost consistent within error ranges for samples collected from 356-, 368-, 414-, and 528-cm depths. In contrast, the other radiocarbon ages appear to be about 4,400–6,500 years older than OSL ages in the depth interval between 50 and 300 cm, and about 1,000–3,300 years older at depths of 350, 400, 500,

Fig. 5 Diagram comprising three panels, **a** grain-size analysis, **b** OSL and radiocarbon ages, and **c** difference between radiocarbon and regressed OSL ages (Δt). The difference between OSL and ^{14}C dates can be interpreted by considering grain-size characteristics (see text for details)



and 550 cm. For samples at 356-, 368-, 414-, and 528-cm depths, OSL ages and radiocarbon ages are in good agreement, suggesting that both OSL and radiocarbon ages may represent the true depositional ages. In addition, eolian sediments are known to be the most suitable materials for OSL dating because the constituent quartz grains have a greater likelihood of being completely bleached by sunlight exposure during transport and upon deposition than do those from other sedimentary environments (Stokes and Gaylord 1993; Stokes et al. 1997). Accordingly, the OSL age results for unit 1 (50–350 cm) and unit 3 (550 cm) are interpreted as directly indicating depositional ages. Thus, the age discrepancy between the OSL and radiocarbon ages in these sediments seems to have resulted from the overestimation of radiocarbon ages.

Overestimation of ^{14}C ages seems most likely to have been caused by incorporation of old reworked carbon into the bulk ^{14}C samples (Grimm et al. 2009). Common sources of ^{14}C -deficient carbon in lakes include detritus from older organic deposits (Nambudiri et al. 1980), bicarbonate and carbonate derived from calcareous bedrock and overburden (Turner et al. 1983), old ground water, which may take millennia to progress through an aquifer and enter a lake (Riggs 1984), and gaseous emissions of ^{14}C -free CO_2 from volcanoes (Olsson 1986). In addition, limnic deposits from recently deglaciated environments are particularly prone to contamination by both old-carbon and hard-water reservoir effects because

the large exposure of unvegetated bedrock and overburden are common sources of ^{14}C -deficient carbon (Sutherland 1980).

Unit 1 (50–300 cm) and unit 3 (550 cm) sediments where the age overestimation is apparent are mainly composed of eolian sediment, and so the effect of inflowing water could be negligible. Also, there is no record of a volcanic eruption in this area during the Pleistocene and Holocene. Therefore, the influence of reworked organic material and airborne inorganic carbon are considered to be the main causes of overestimation of radiocarbon ages in units 1 and 3. Paleozoic limestones and dolomites are widely distributed to the west and south of the lake, and the westerly is dominant in the study area. During our field work in summer 2007, frequent eolian dust events caused by strong west winds were observed. Accordingly, the overestimation of radiocarbon dates in the 50–300 cm depth interval and in the 550-cm horizon is interpreted to be a result of high eolian inputs of soil material and detrital carbonate from carbonate rocks to the west of the studied lake. However, at depths of 356 and 368 cm, ^{14}C and OSL ages are in agreement. Although the mean grain size remains similar within unit 1, the weight percent of TOC (total organic carbon) and CaCO_3 are highest in the interval between 340 and 394 cm (Lee et al. 2009), which indicates humid paleoclimates in the study area between about 11,170 and 9,620 cal years BP based on our OSL ages. Such humid conditions were also inferred from Bayan Nuur (Lake), western

Mongolia, which had highest lake levels between $11,230 \pm 60$ years BP and $9,690$ years BP (Grunert et al. 2000). Under relatively humid conditions, the influence of detrital carbonate was probably not important, suggesting that radiocarbon ages at 356 and 368 cm could be close to the true ages. In the case of the sediment at 350-cm depth, the influence of ^{14}C -deficient carbon was maintained by eolian sedimentation during a transitional period in which paleoclimate changed from humid toward relatively arid conditions. The overestimation of radiocarbon ages compared with OSL ages (at 400- and 500-cm depths) in unit 2 sediments can be attributed to the addition of old carbon by intermittent glaciofluvial processes. Two radiocarbon ages that agree with OSL ages at 414- and 528-cm depths have relatively small mean grain sizes ($\sim 7 \varphi$) in unit 2 and are interpreted to have been less affected by glaciofluvial sediment.

The difference between radiocarbon ages and regressed OSL ages (Δt) at the same core depth may indicate how much ^{14}C -deficient carbon was delivered into Lake Ulaan (Fig. 5c). The sediments of Lake Ulaan were more ^{14}C deficient during the mid-to late Holocene (~ 50 –300 cm depth interval) than during the late Pleistocene. Δt is larger during the Holocene (4,100–5,800 years) than during the Pleistocene (2,700–3,000 years), suggesting that eolian activity during the Holocene was more influential than during the late Pleistocene. This may be because land surface was partially covered by snow and/or ice in the Pleistocene. The minimum Δt value, which indicates the minimum influence from old reworked carbon, appears around the Pleistocene–Holocene boundary (about 350-cm depth). Considering that the eolian activity had the most influence on the ^{14}C age overestimation in the studied lake, the Pleistocene–Holocene boundary is regarded to be the most humid time in southern Mongolia.

Conclusions

A chronology for a 5.88-m-long sediment core taken from Lake Ulaan is presented based on radiocarbon and OSL dating methods. Comparison of OSL ages with ^{14}C ages shows poor agreement except for a few samples. Based on the fact that eolian processes were the dominant means of sediment deposition, the results from OSL dating may provide the more

reliable geochronological framework of the studied core spanning the last 16,000 years. Bulk ^{14}C ages agree with OSL ages around the Pleistocene–Holocene boundary, but are generally about 4,100–5,800 years (during the Holocene) and 2,700–3,000 years (during the late Pleistocene) older than the corresponding OSL ages. Because eolian and glaciofluvial input of old organic material and detrital carbonate were the main reasons for the overestimation of radiocarbon ages for this study, the age difference between the OSL and radiocarbon ages is interpreted to reflect mainly the strength of eolian activity. The results of this study reveal that the application of OSL dating method to lacustrine sediments has a greater potential than the radiocarbon dating method, especially in the regions where eolian sedimentation is dominant.

Acknowledgments This work was supported by the Korea Polar Research Institute Project (PE10010), the Korea Meteorological Administration Research and Development Program (RACS 2010-3007, PN10040), and partly by a SNU-SEES BK21 program.

References

- Aravena R, Warner B, MacDonald GM, Hanf KI (1992) Carbon isotope composition of lake sediments in relation to lake productivity and radiocarbon dating. *Quat Res* 37:333–345
- Bøtter-Jensen L, Bulur E, Duller GAT, Murray AS (2000) Advances in luminescence instrument systems. *Radiat Meas* 32:523–528
- Clayton L, Moran SR (1982) Chronology of late Wisconsin glaciations in middle North America. *Quat Sci Rev* 1:55–82
- Fowler AJ, Gillespie R, Hedges REM (1986) Radiocarbon dating of sediments. *Radiocarbon* 28:441–450
- Grimm EC, Maher LJ Jr, Nelson DM (2009) The magnitude of error in conventional bulk-sediment radiocarbon dates from central North America. *Quat Res* 72:301–308
- Grunert J, Lehmkuhl F, Walther M (2000) Paleoclimatic evolution of theUvs Nuur basin and adjacent areas (Western Mongolia). *Quat Int* 65/66:171–192
- Jones KPN, McCave IN, Patel PD (1988) A computer interfaced sedigraph for modal size analysis of fine-grained sediment. *Sedimentology* 35:163–172
- Karrow PF, Anderson TW (1975) Palynological study of lake sediment profiles from southwestern New Brunswick: discussion. *Can J Earth Sci* 12:1808–1812
- Lee MK, Lee YI, Lim HS, Lee JI, Yoon HI (2009) Climatic changes during the Holocene and late Pleistocene recorded in Ulaan Lake sediments, Mongolia. In: Proceedings of the 64th annual meeting geological society Korea 64, p 60

- Liu XJ, Lai ZP, Fan QS, Long H, Sun YJ (2010) Timing for high lake levels of Qinghai Lake in the Qinghai-Tibetan Plateau since the last interglaciation based on quartz OSL dating. *Quat Geochronol* 5:218–222
- Long H, Lai ZP, Wang NA, Zhang JR (2011) A combined luminescence and radiocarbon dating study of Holocene lacustrine sediments from arid northern China. *Quat Geochronol* 6:1–9
- MacDonald GM, Beuken RP, Kieser WE, Vitt DH (1987) Comparative radiocarbon dating of terrestrial plant macrofossils and aquatic moss from the “ice-free corridor” of western Canada. *Geology* 15:837–840
- Murray AS, Wintle AG (2000) Luminescence dating of quartz using an improved single-aliquot regenerative-dose protocol. *Radiat Meas* 32:57–73
- Murray AS, Wintle AG (2003) The single aliquot of regenerative dose protocol: potential for improvements in reliability. *Radiat Meas* 37:377–381
- Murray AS, Marten R, Johnston A, Martin P (1987) Analysis for naturally occurring radionuclides at environmental concentrations by gamma spectrometry. *J Radioanal Nucl Chem* 115:263–288
- Nambudiri EMV, Teller JT, Last WM (1980) Pre-quaternary microfossils—a guide to errors in radiocarbon dating. *Geology* 8:123–126
- Olley JM, Murray AS, Roberts RG (1996) The effects of disequilibria in the uranium and thorium decay chains on burial dose rates in fluvial sediments. *Quat Sci Rev* 15:751–760
- Olsson IU (1986) Radiometric dating. In: Berglund BE (ed) *Handbook of Holocene palaeoecology and palaeohydrology*. John Wiley & Sons, Chichester, pp 273–312
- Prescott JR, Hutton JT (1988) Cosmic ray and gamma ray dosimetry for TL and ESR. *Int J Radiat Appl Instrum Part D Nucl Tracks Radiat Meas* 14:223–227
- Prescott JR, Hutton JT (1994) Cosmic ray contributions to dose rates for luminescence and ESR dating: large depths and long-term time variations. *Radiat Meas* 23:497–500
- Ramsey CB (2009) Bayesian analysis of radiocarbon dates. *Radiocarbon* 51:337–360
- Rees-Jones J (1995) Optical dating of young sediments using fine-grain quartz. *Anc TL* 13:9–14
- Reimer PJ, Baillie MGL, Bard E, Bayliss A, Beck JW, Blackwell PG, Ramsey CB, Buck CE, Burr GS, Edwards RL, Friedrich M, Grootes PM, Guilderson TP, Hajdas I, Heaton TJ, Hogg AG, Hughen KA, Kaiser KF, Kromer B, McCormac FG, Manning SW, Reimer RW, Richards DA, Southon JR, Talamo S, Turney CSM, van der Plicht J, Weyhenmeyer CE (2009) IntCal09 and marine09 radiocarbon age calibration curves, 0–50,000 years CAL BP. *Radiocarbon* 51:1111–1150
- Riggs AC (1984) Major carbon-14 deficiency in modern snail shells from southern Nevada springs. *Science* 224:58–61
- Schidlowski M, Hayes JM, Kaplan IR (1983) Isotopic inferences of ancient biochemistries: carbon, sulfur, hydrogen and nitrogen. In: Schopf JW (ed) *Earth’s earliest biosphere: its origin and evolution*. Princeton University Press, Princeton, pp 149–186
- Sevastyanov DV, Dorofeyk NI (2005) A short review: limnological and paleolimnological researches in Mongolia carried out by joint Russian-Mongolian expeditions. *J Mt Sci* 2:86–90
- Shen Z, Mauz B, Lang A, Bloemendal J, Dearing J (2007) Optical dating of Holocene lake sediments: elimination of the feldspar component in fine silt quartz samples. *Quat Geochronol* 2:150–154
- Stokes S, Gaylord DR (1993) Optical dating of Holocene dune sands in the Ferris Dune Field, Wyoming. *Quat Res* 39:274–281
- Stokes S, Thomas DSG, Washington R (1997) Multiple episodes of aridity in southern Africa since the last interglacial period. *Nature* 388:154–158
- Sutherland DG (1980) Problems of radiocarbon dating in newly deglaciated terrain: examples from the Scottish Lateglacial. In: Lowe JJ, Gray JM, Robinson JE (eds) *Studies in the Lateglacial of north-west Europe*. Pergamon, Oxford, pp 139–149
- Telford RJ, Heegaard E, Birks HJB (2004) The intercept is a poor estimate of a calibrated radiocarbon age. *Holocene* 14:296–298
- Turner JV, Fritz P, Karrow PF, Warner BG (1983) Isotopic and geochemical composition of marl lake waters and implications for radiocarbon dating of marl lake sediments. *Can J Earth Sci* 20:599–615
- Wintle AG, Murray AS (2006) A review of quartz optically stimulated luminescence characteristics and their relevance in single-aliquot regeneration dating protocols. *Radiat Meas* 41:369–391
- Zhao H, Lu Y, Wang C, Chen J, Liu J, Mao H (2010) ReOSL dating of aeolian and fluvial sediments from Nihewan Basin, northern China and its environmental application. *Quat Geochronol* 5:159–163
- Zimmerman DW (1971) Thermoluminescence dating using fine grains from pottery. *Archaeometry* 13:29–52